fibers

MDPI

Article

Improving the Surface Quality of FDM 3D-Printed Wood–PLA Composites Through CNC Milling

Wojciech Jasiński *, Karol Szymanowski and Piotr Borysiuk *

Institute of Wood Sciences and Furniture, Warsaw University of Life Sciences-SGGW, 159 Nowoursynowska St., 02-776 Warsaw, Poland; karol_szymanowski@sggw.edu.pl
* Correspondence: 9.wojciech.jasinski@gmail.com (W.J.); piotr_borysiuk@sggw.edu.pl (P.B.)

Highlights

What are the main findings?

- Wood–PLA composites exhibited higher surface roughness than neat polymers.
- CNC milling substantially reduced the surface roughness of all investigated wood–PLA composites.
- Lower cutting forces were recorded for wood–PLA composites than for neat PLA and ASA.
- Print orientation affected surface roughness and, to a lesser extent, cutting forces.

What are the implications of the main findings?

- CNC milling offers an effective post-processing approach for improving the surface quality of FDM-printed wood–PLA composites.
- The layered structure of FDM-printed composites should be considered during CNC milling to avoid surface damage and deterioration of surface quality.

Abstract

Additive manufacturing enables the production of complex components, but the layered deposition process can result in pronounced surface irregularities, particularly when wood particles are incorporated into the polymer matrix. This study investigates the mechanical performance and surface characteristics of wood–PLA materials and evaluates CNC milling as a post-processing method. Three wood–PLA composites, PLA, and ASA, were examined. Tensile and flexural properties as well as density were determined for the investigated materials. Cutting forces were measured during milling, while surface roughness was evaluated before and after milling for specimens produced in different orientations. The wood–PLA composites exhibited lower mechanical properties than neat PLA, with tensile strength reduced by 24–43% and flexural strength by 36–57%. Internal voids and imperfect fusion between deposited strands were identified as important factors affecting the measured performance. Their initial roughness was higher than that of the neat polymers, indicating a substantial contribution from material heterogeneity. Milling substantially reduced roughness for all wood–PLA composites and required cutting forces up to 48% lower than the neat polymers under the investigated conditions. CNC milling therefore constitutes an effective approach for improving the surface quality of these materials, although machining parameters should be selected with their layered structure in mind.

Keywords: extrusion; additive manufacturing; WPC; surface roughness; machinability; cutting forces; post-processing

Check for updates

Academic Editor: Peter Niemz

Received: 26 September 2026
Revised: 22 October 2026
Accepted: 2 November 2026
Published: 4 November 2026

Copyright: © 2026 by the authors. Licensee MDPI, Basel, Switzerland. This article is an open access article distributed under the terms and conditions of the Creative Commons Attribution (CC BY) license.

1. Introduction

Fused deposition modelling (FDM), also referred to as fused filament fabrication (FFF), is an additive manufacturing technology in which thermoplastic material is deposited layer by layer to produce components with complex geometries without the need for conventional tooling. The process offers considerable flexibility in the fabrication of customised and low-volume components. However, the layer-by-layer deposition of material also results in characteristic surface irregularities and anisotropic properties. The final surface characteristics depend on both the geometry of the deposited material and the processing conditions, making surface quality one of the important limitations when FDM-printed components are intended for functional or visually demanding applications [1,2].

The use of wood particles or fibres as fillers in thermoplastic filaments has expanded the range of materials available for FDM and provides an opportunity to combine the processability of thermoplastics with the renewable origin and characteristic appearance of wood-based materials [3,4]. In particular, wood–PLA composites have been investigated extensively with respect to their mechanical properties, printability, microstructure, and processing conditions. The addition of wood particles, however, introduces material heterogeneity that can affect melt flow, interfacial bonding, porosity, and the quality of the resulting printed surface [4–6]. Previous studies have shown that increasing wood content can increase the surface roughness of printed parts and contribute to the formation of internal voids and visible clusters of wood particles [5]. The structure and processing of wood-filled filament can also affect porosity and the properties of the printed material [6]. In particular, higher wood content was associated with increased filament roughness and porosity, whereas thermal modification of the wood particles reduced both characteristics and improved the tensile strength of printed parts relative to those containing unmodified wood particles at the same filler content [6]. The surface roughness of FDM-printed wood–PLA materials has also been reported to increase with increasing layer thickness. In particular, comparisons of different layer thicknesses have shown that thinner layers generally produce smoother surfaces, highlighting the importance of deposition settings in controlling surface quality [7]. More recently, systematic studies have examined the effects of material type and selected printing parameters on the surface roughness of PLA-based and wood-filled PLA filaments, confirming that both material characteristics and printing conditions can contribute to surface quality [8].

The surface structure generated by FDM can subsequently be modified by subtractive post-processing. CNC machining is an established approach for improving the dimensional accuracy and surface finish of polymeric FDM components, and previous studies have demonstrated that milling can substantially reduce the surface roughness of printed PLA parts [2]. The effect of build orientation on the surface before and after machining has also been investigated, showing that the anisotropic surface structure associated with material deposition can influence the resulting roughness [2]. In parallel, the machining of conventional wood–plastic composites has been investigated with respect to cutting parameters and their effects on surface roughness, demonstrating that parameters such as spindle speed, feed rate, and milling depth can significantly affect the machined surface [9]. These studies indicate that both the heterogeneous composition of wood–plastic materials and the process-induced structure of additively manufactured parts can be relevant to the resulting surface characteristics.

Despite these developments, the available literature provides limited information on the CNC machining of FDM-printed wood–PLA composites. Existing studies have largely considered either the formation and optimisation of the surface of wood-containing FDM materials [5–8] or the machining of conventional FDM polymers [2] and wood–plastic composites manufactured by other processes [9]. Consequently, the interaction between the

characteristic layer and strand-based structure produced by FDM and the heterogeneous structure introduced by wood particles during subsequent milling remains insufficiently explored. In particular, limited attention has been given to whether CNC milling affects only the overall level of surface roughness or also the pronounced profile extremities that may occur on wood-filled FDM surfaces. This issue is relevant because the surface of an FDM-printed wood–PLA component is determined not only by the deposition process but also by the spatial distribution and interfacial behaviour of the wood phase. A better understanding of the response of such surfaces to CNC milling is therefore important for assessing the suitability of subtractive post-processing for improving the surface characteristics of wood-filled FDM components. This study addresses this gap by experimentally evaluating the changes in surface roughness of FDM-printed wood–PLA composites following CNC milling and comparing the results with those obtained for neat PLA and ASA. The study also examines cutting forces and the influence of print orientation on these forces, providing a comparative analysis of surface quality improvement and cutting forces across the investigated materials.

2. Materials and Methods

Three commercial wood–PLA composites and two common FDM filaments, PLA and ASA (Spectrum Filaments, Pęcice Małe, Poland; ROSA PLAST Sp. z o.o., Hipolitów, Poland; Fiberlogy, Brzezie, Poland), were used in this study. The manufacturer-provided properties of those materials, are shown in Table 1. Where possible, filaments with natural colour were chosen to limit the possible impact of pigments on tested properties. The investigated wood–PLA composites were commercially available filaments with proprietary formulations. Detailed information on wood content, particle size distribution, and filler morphology was not provided by the manufacturers. Therefore, the composites were treated as distinct commercial materials rather than formulations with controlled wood content. Consequently, differences between the composites cannot be directly attributed to specific compositional characteristics.

Table 1. Typical properties of materials used in this study as provided by manufacturers [10–14].

Material	Density [g/cm^3]	Tensile Strength [MPa]	Tensile Modulus [MPa]	Maximum Operating Temperature [°C]
PLA	1.24	53	3495	$55_{(HDT)}$
ASA	1.07	43	2500	$96_{(VICAT)}$
Composite A	1.26	34	3195	$50_{(VICAT)}$
Composite B	1.30	27	3600	$50_{(HDT)}$
Composite C	1.15	47	2900	not provided

Those materials were used to 3D print samples described further using a Voron 2.4 (Voron Design, Panama City, FL, USA) FDM 3D printer equipped with a Dragon HF (Phaetus 3D Technology, Suzhou, China) hotend and a hardened steel 0.8 mm nozzle. All of the printed samples were modelled in Fusion 360 v.2604.1.48 (Autodesk, San Francisco, CA, USA) and converted to g-code using Prusa Slicer 2.6.1 (Prusa Research, Prague, Czech Republic). Material-specific settings (nozzle and bed temperatures, extrusion multiplier, pressure advance, cooling) were chosen separately for each material according to procedures recommended by the 3D printer's manufacturer [15] and are shown in Table 2. These settings are specific to the material–machine combination and are reported to document

the conditions used in this study. Those should not be considered as universal values or a substitute for appropriate calibration when using other materials or equipment. The number of walls was set at the maximum value to obtain fully solid, non-hollow samples with extrusion lines parallel to the forces applied during testing and eliminate the impact of different infill structures and densities. A layer height of 0.3 mm was chosen. Other settings were kept as provided by the slicer's manufacturer for this specific printer model. Prior to printing, filaments were dried to a constant mass using Sunlu Filadryer S2 (Sunlu International Holdings Limited, Montauk, NY, USA) set at 50 °C.

Table 2. Material-specific print settings used in this study.

Material	Nozzle Temperature [°C]	Bed Temperature [°C]	Extrusion Multiplier [-]	Pressure Advance [-]	Print Cooling [%]
PLA	210	60	0.96	0.013	100
ASA	245	95	0.91	0.015	20
Composite A	200	60	0.94	0.010	100
Composite B	200	60	0.92	0.010	100
Composite C	200	60	0.96	0.012	100

To evaluate the physicomechanical properties of 3D-printed materials, the following tests were performed:

- Density according to EN 323 [16];
- Tensile strength and tensile modulus according to ISO 527 [17];
- Flexural strength and flexural modulus according to ISO 178 [18].

All tests mentioned above involved ten repetitions. The tensile tests utilised 3D-printed samples of ISO 527 Type 1A (Figure 1a). The flexural and density tests utilised 3D-printed samples of shape and dimensions described in ISO 178 (Figure 1b). The aforementioned procedures were chosen based on EN 15534 [19].

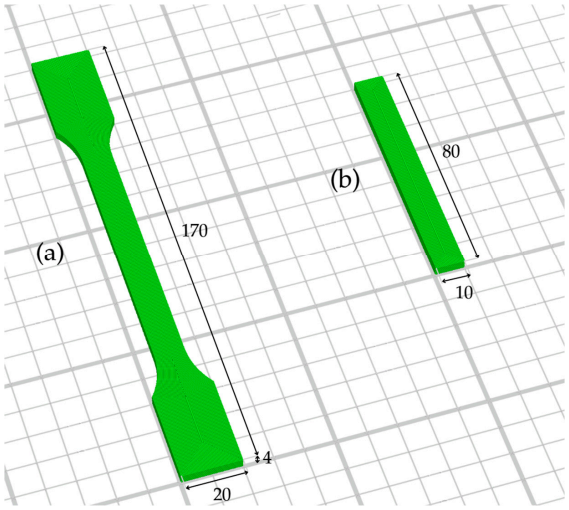

Figure 1. Specimens used in physicomechanical tests (units in mm): (**a**) ISO 527 Type 1A; (**b**) ISO 178.

Due to the anisotropic structure of 3D-printed objects, specimens for CNC machining and surface roughness testing were printed in two orientations, with the test surface being either parallel (Figure 2a) or perpendicular (Figure 2b) to the 3D printer's bed, further indicated by the symbols "∥" and "⊥" respectively. Five samples for each material and print

orientation were machined using the Busellato JET130 CNC machining centre (Casadei Busellato, Thiene, Italy). A two-flute 6 mm helix square endmill was used with a cutting depth set at 5 mm. A tool speed (n) of 18,000 revolutions/min and a feed (v) of 3.6 m/min were chosen experimentally, resulting in a feed-per-tooth (f_z) of 0.1 mm. Cutting paths were prepared so as to utilise the full width of the endmill. During machining, forces parallel to the feed direction were measured. The test setup including the measurement chain used is shown in Figure 3.

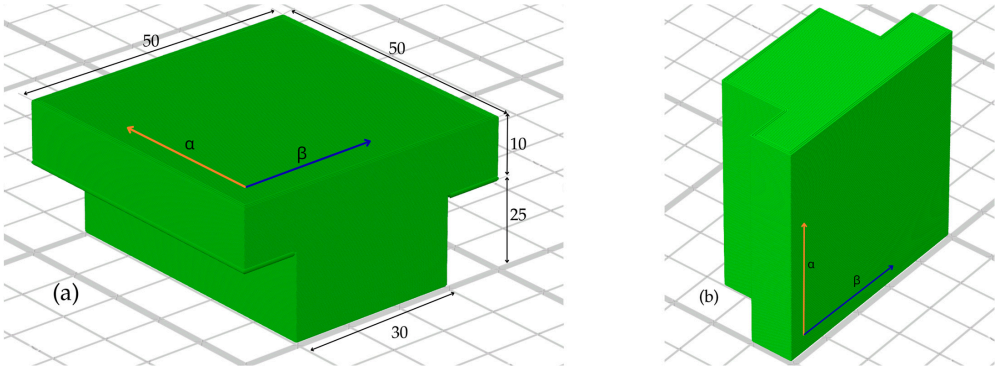

Figure 2. Specimens used in machining and surface roughness tests and their print orientations (units in mm): (**a**) parallel to the print bed (∥); (**b**) perpendicular to the print bed (⊥); α, β—directions in which surface roughness was measured.

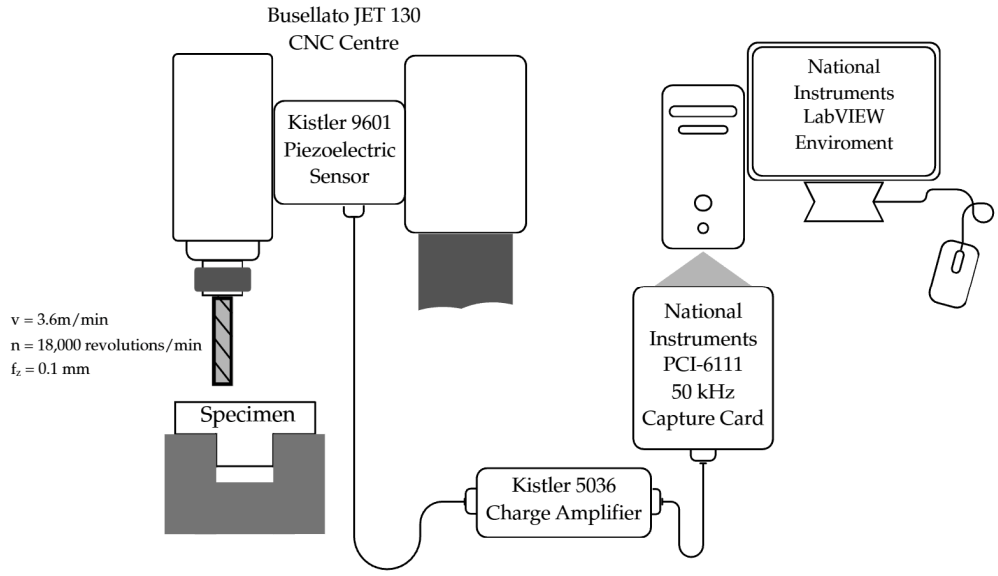

Figure 3. Machining setup.

Surface roughness was tested prior to and after machining using Mitutoyo SJ-201 (Mitutoyo Corporation, Sakado, Japan) in standalone mode according to the manufacturer's instructions. Four different values were recorded for each measurement—arithmetic roughness average (Ra), mean roughness depth (Rz), maximum profile height (Ry) and root mean square average roughness (Rq). Ra was measured for ease of comparison, as it is the most prevalent parameter used to describe surface roughness. Rq was used for statistical analysis, while Rz and Ry allowed for fuller description of surface quality in terms of profile extremities. The parameters described above were measured in two directions, perpendicular to the edges of the measured surface and each other, denoted as "α" and "β" as shown in Figure 2. For machined samples, measurements only in "α" direction were performed due to material left between machining passes.

To evaluate the significance of differences, ANOVA (Analysis of variance) with post hoc Tukey tests were performed in STATISTICA 13 (TIBCO Software Inc., Palo Alto, CA, USA) with a confidence level of 0.95.

3. Results and Discussion

3.1. Physicomechanical Characterisation

The results of the tensile strength tests are shown in Figure 4. Composites A (23.9 MPa) and B (22.84 MPa) display no significant differences, similarly to PLA (39.95 MPa) and ASA (36.91 MPa). The results obtained for composite C (30.18 MPa) are higher than those obtained for composites A and B; however they are still significantly lower than the results obtained for non-filled materials. While overall trends, such as the tensile strength of composite C being lower than the tensile strength of both neat filaments and the tensile strength of PLA being higher than the tensile strength of ASA, conform to expectations based on data provided by the materials' manufacturers (Table 1), all of the values are significantly lower than expected.

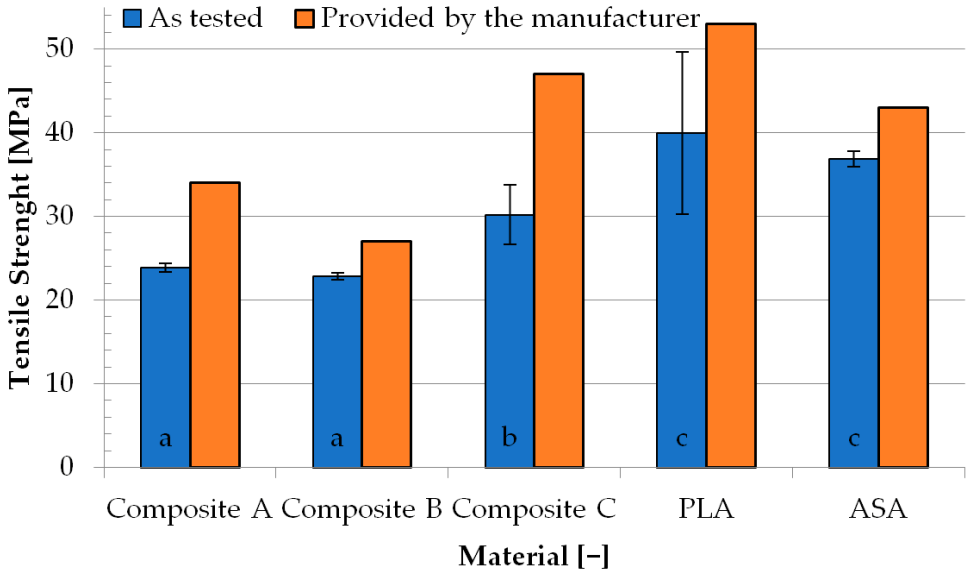

Figure 4. Tensile strength of the tested materials; a–c—homogeneous groups.

The tensile modulus test results (Table 3) show similar trends to the tensile strength results. No significant differences between the three tested composites could be found in this test. The results for PLA are the highest in this test, while ASA displays the lowest value obtained. Differences between values obtained during tensile testing and typical values provided by the manufacturer are even more pronounced than differences in tensile strength. Th experimental results are from 2.8 to 3.2 times lower than the expected, typical values.

The results of the flexural strength tests are shown in Table 4. Composites A and B display a small but statistically significant difference, while composite C exhibits higher flexural strength than both of those. The values obtained for all three composites remain lower than those measured for the non-filled materials. PLA demonstrates the highest flexural strength, whereas ASA shows a lower yet still markedly higher value than the tested composites. The flexural modulus results follow similar trends. Two of the composites show comparable stiffness, with values of 1999 MPa (composite A) and 2043 MPa (composite C), with no significant differences between them. The flexural modulus obtained for composite B (2424 MPa) is higher than that of both other composites. PLA exhibits the highest

modulus, while ASA presents the lowest modulus among the tested materials. Overall, the neat polymers display superior flexural performance compared to the composite variants.

Table 3. Tensile modulus of the tested materials.

Material	Tensile Modulus [MPa]	Typical Tensile Modulus * [MPa]
Composite A	1010 [a]	3195
Composite B	1095 [a]	3600
Composite C	1080 [a]	2900
PLA	1216 [b]	3495
ASA	889 [c]	2500

*—provided by the manufacturer; [a,b,c]—homogeneous groups.

Table 4. Flexural properties of the tested materials.

Material	Flexural Strength [MPa]	Flexural Modulus [MPa]
Composite A	48.36 [a]	1999 [A]
Composite B	45.12 [b]	2424 [B]
Composite C	66.84 [c]	2043 [A]
PLA	103.98 [d]	2805 [C]
ASA	70.74 [e]	1709 [D]

[a,b,c,d,e,A,B,C,D]—homogeneous groups.

No manufacturer-provided data is available regarding flexural properties of the tested materials. Flexural strength values for both PLA and ASA measured in this study are consistent with those reported in the literature [20,21]. However, discrepancies are observed in the flexural modulus results. The flexural modulus of PLA is reported to be 3500 MPa, whereas the value obtained in this study was 2805 MPa [20]. Similarly, the reported flexural modulus for ASA is approximately 2210 MPa, compared to 1709 MPa measured during testing [21].

Differences observed in both tensile properties and the flexural modulus can be attributed to the internal structure of 3D-printed components (Figure 5). Although the specimens in this study were printed using parameters intended to produce fully solid parts, FDM-printed components are inherently composed of deposited strands that may not be perfectly fused, resulting in internal voids. Imperfect interlayer bonding and variability in filament extrusion can result in non-uniform stress distribution across the specimen cross-section, contributing to the reduced mechanical properties observed in this study.

Observation of cross-sections of samples after flexural tests, as illustrated in Figure 6, shows both imperfect fusion of deposited strands and internal voids, which are the most probable reason for differences between expected and obtained results.

The densities of the printed samples (Figure 7), similarly to other mechanical tests, show discrepancies between values obtained during the study and values expected based on manufacturer-provided data, implying the existence of internal voids in the printed samples as described above. Composites B (1049 kg/m^3) and C (1053 kg/m^3) show similar density, while all other differences between the tested materials are statistically significant. The density of composite A (1009 kg/m^3) is lower than values obtained for other WPCs, while the density of ASA (943 kg/m^3) is the lowest among all tested materials. The values obtained for PLA (1126 kg/m^3) are the highest in this test.

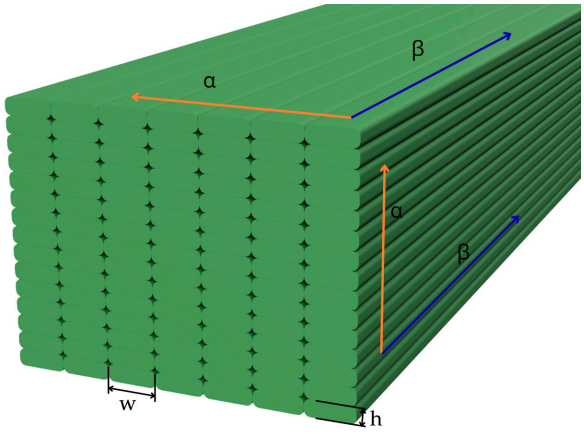

Figure 5. Theoretical structure of 3D-printed objects; h—layer height; w—extrusion width; α, β—directions in which surface roughness was measured.

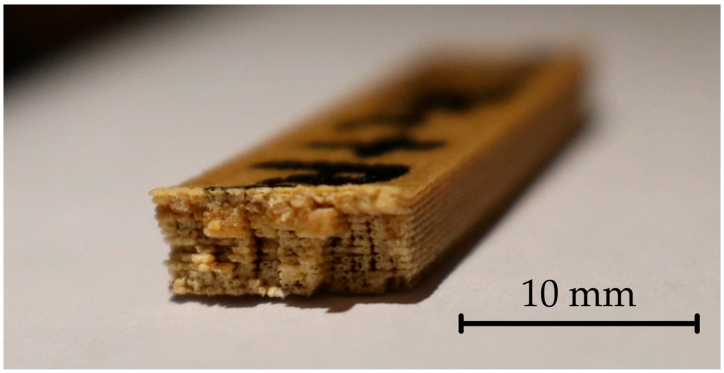

Figure 6. Cross-section of composite C sample after flexural tests.

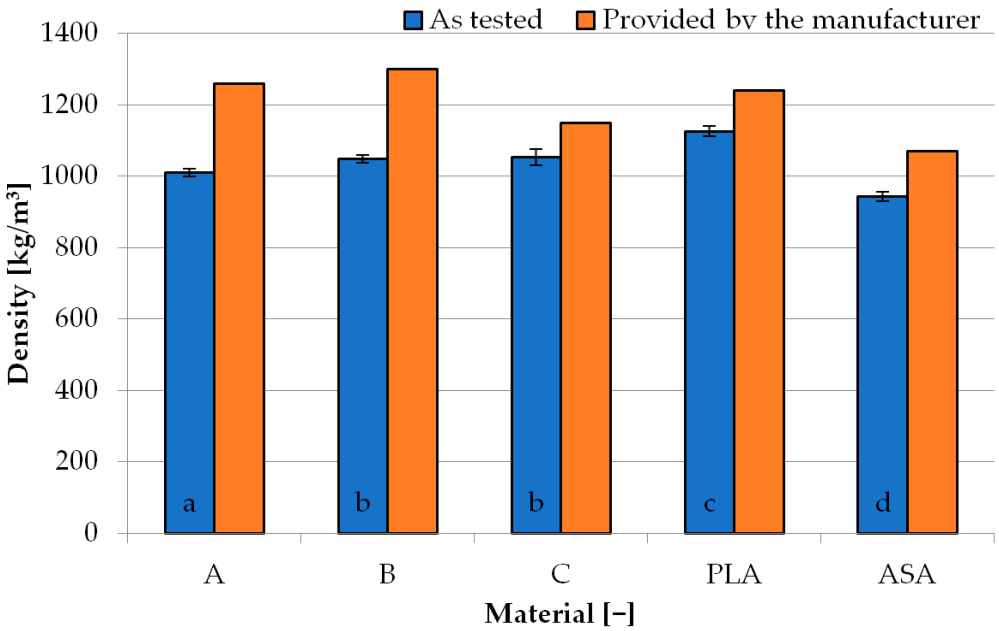

Figure 7. Density of the tested materials; a–d—homogeneous groups.

The differences described above highlight the challenges associated with the lack of standardised testing protocols for 3D-printed components. Both manufacturers and the cited authors utilised pressed, extruded, or injection-moulded specimens, as ISO 178 does not permit the use of 3D-printed samples. The manufacturing method and specimen

preparation can substantially affect the obtained results. In particular, FDM introduces a characteristic layered structure, interlayer interfaces and process-induced porosity that are not present in the same form in conventionally moulded materials [4]. This difference is particularly relevant for composites, for which the morphology, size and distribution of the particles, as well as the quality of the interface, can affect the mechanical performance of the printed parts [22]. Krapež Tomec et al. [6] reported that injection-moulded specimens exhibited 18–69% higher tensile strength than corresponding 3D-printed specimens, depending on the composite formulation, demonstrating the substantial influence of the manufacturing process on the resulting mechanical properties. Therefore, mechanical properties reported for conventionally manufactured wood–polymer composites should be compared with FDM results with caution, as differences in material structure and processing may contribute substantially to the observed values.

Potential approaches to improving the mechanical performance of FDM-printed wood–PLA composites include reducing internal porosity, improving interlayer bonding, enhancing adhesion between wood particles and the polymer matrix, and optimising filler characteristics and processing parameters. However, such modifications require further experimental investigation, particularly because changes in printing temperature may also affect the thermal stability of the wood component.

3.2. Machining and Surface Roughness

The results of the cutting force measurements during machining are presented in Figure 8. The lowest cutting forces were recorded for composite B, with values of 15.50 N when printed parallel to the bed and 17.55 N when printed perpendicular to the bed, indicating a noticeable influence of print orientation. Similarly low values were observed for composite C, particularly when printed perpendicular to the bed (17.21 N), while printing parallel resulted in a slightly higher force (18.48 N). Composite A showed comparable results regardless of orientation, with forces of 19.03 N (parallel) and 19.12 N (perpendicular), indicating limited influence of printing direction for this material.

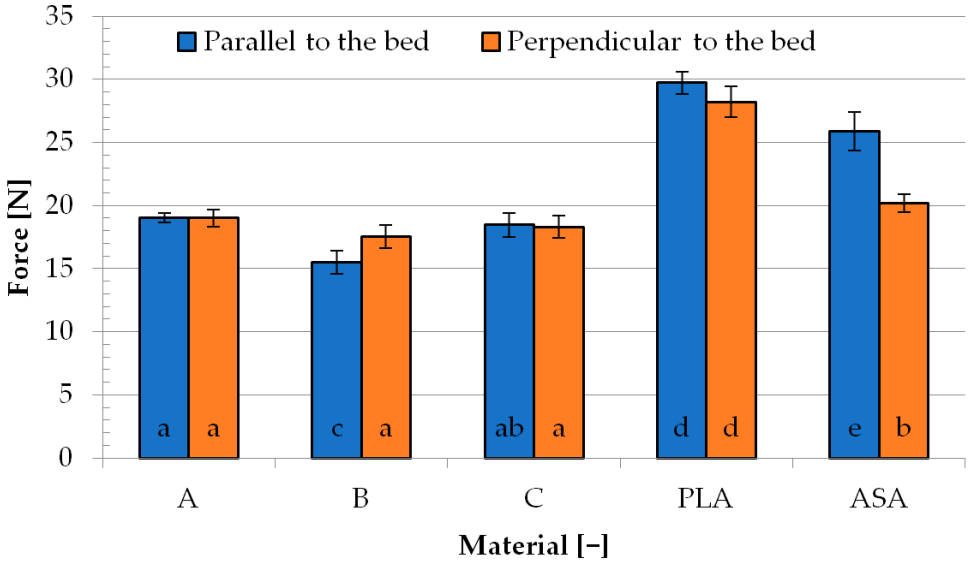

Figure 8. Forces during machining of the tested materials; a–e—homogeneous groups.

For the neat polymers, higher forces were generally required. PLA exhibited the highest cutting forces, reaching 28.20 N when printed perpendicular to the bed and 29.75 N when printed parallel. ASA printed parallel to the bed also showed relatively high forces

(25.87 N). However, ASA printed perpendicular to the bed produced a noticeably lower value (20.22 N), closer to those obtained for the composite materials.

Overall, the composites required lower machining forces than the neat polymers. Printing orientation had a more pronounced effect on the results for ASA than for the other materials, which may be attributed to the relatively low interlayer adhesion of ASA filaments [23].

The lower cutting forces observed for the wood–PLA composites compared with the neat polymers indicate lower mechanical loading of the cutting tool and the machine-tool system under the investigated conditions. As shown by the mechanical tests, all three composites exhibited lower tensile and flexural strength than PLA, as well as lower tensile and flexural moduli. Their lower mechanical resistance may contribute to the lower forces required for material removal during milling. From the perspective of machining, the lower cutting forces indicate that less mechanical effort is required to remove material, resulting in lower loading of the cutting tool and the machine-tool system. Thus, the wood–PLA composites exhibited more favourable machining behaviour than the neat polymers in terms of cutting forces under the applied conditions. The effect of print orientation on cutting forces was less pronounced for the wood–PLA composites than for ASA. It should be noted, however, that despite the relatively favourable machining response observed under the applied cutting conditions, the layer-based structure of these materials requires careful selection of machining parameters. Milling too close to the boundaries between deposited layers may result in the tear out of thin remnants of the machined material, particularly when the remaining section is insufficient to withstand the cutting forces. This can lead to substantial deterioration of the machined surface, as the thin portions of the printed layer may be torn away rather than cleanly cut. Such behaviour was observed during preliminary machining tests, before the cutting parameters were optimised, and is presented in Figure 9. Although lower cutting forces were recorded for the wood–PLA composites, these results should not be interpreted as evidence of superior overall machinability. A comprehensive assessment would require additional investigation of tool wear, surface integrity, chip formation, and machining performance under different cutting conditions.

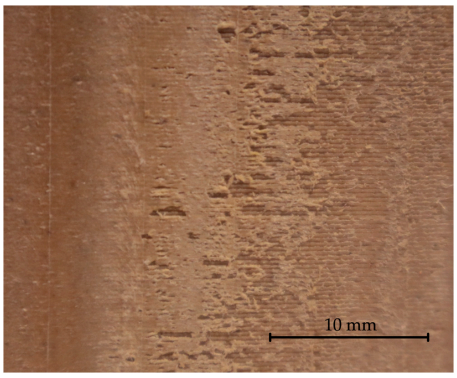

Figure 9. Surface damage during milling in preliminary machining tests.

Surface roughness (Rq) results for specimens before machining are presented in Figure 10. In all cases, higher roughness values were recorded in the α direction compared to β. For composite A, Rq decreased from 19.6 to 12.1 for parallel orientation and from 30.9 to 21.7 for perpendicular orientation when comparing α to β. A similar trend was observed for composite B, with values decreasing from 22.7 to 19.0 (parallel) and from 26.9 to 21.7 (perpendicular). Composite C also followed this pattern, with reductions from 16.9 to 13.5 and from 24.1 to 14.4 for parallel and perpendicular orientations, respectively. For the neat polymers, PLA exhibited a notable reduction from 10.4 to 5.7 (parallel) and from 19.5

to 2.0 (perpendicular), while ASA showed decreases from 9.2 to 4.1 and from 20.7 to 2.6. The differences between α and β were particularly pronounced for PLA and ASA in the perpendicular orientation. Overall, the α direction consistently yielded higher roughness values, with the magnitude of directional differences depending on both material type and print orientation.

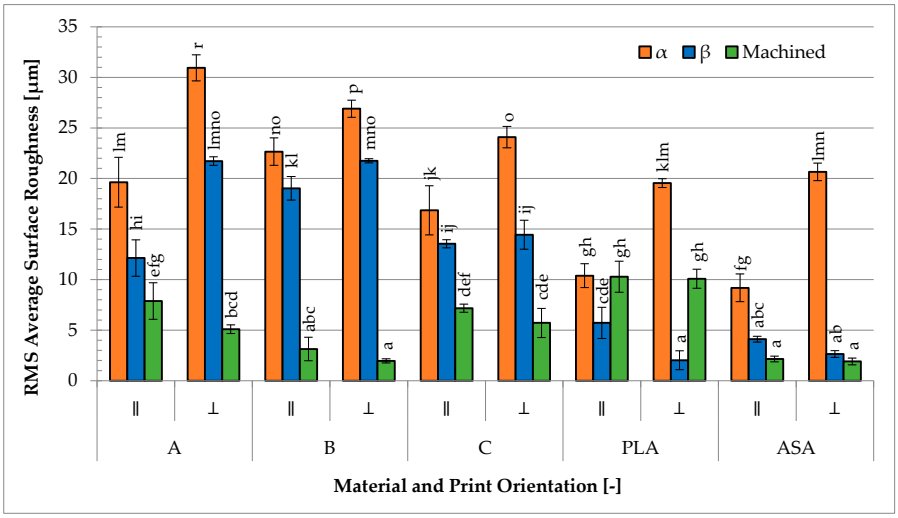

Figure 10. Rq of the tested materials before and after machining. a–p,r—homogeneous groups; ∥, ⊥—print orientation.

These differences can be attributed to the anisotropic structure of 3D-printed components. Measurements in the α direction were performed perpendicular to the print lines, which were formed either by the discrete layers (⊥) or by the deposited strands within each layer (∥), while measurements in the β direction were performed parallel to these lines. The print lines described above are readily distinguishable on the specimen surfaces (Figure 11). Visual comparison of the specimen surfaces indicates that the surface roughness of components printed from neat polymers is primarily a result of the 3D printing process. Consequently, it may be possible to reduce the surface roughness of those materials through optimisation of the printing parameters, which is also supported by the surface roughness measurements obtained in this study. In contrast, both the visual comparison and roughness measurements indicate that the incorporation of wood particles into the polymer matrix results in a worse surface quality in both measurement directions. These findings suggest that material-related factors may contribute to the higher surface roughness of wood–PLA composites in addition to the effects of printing parameters. However, the extent to which surface roughness could be reduced through further optimisation of printing conditions was not investigated in the present study.

Machining led to a substantial reduction in surface roughness for all composite materials. For composite A, Rq decreased from 19.6 to 7.9 in the parallel orientation and from 30.9 to 5.1 in the perpendicular orientation. Composite B exhibited an even greater reduction, from 22.7 to 3.1 (parallel) and from 26.9 to 2.0 (perpendicular), representing the lowest roughness values among all tested composites after machining. Composite C showed similar improvements, with values decreasing from 16.9 to 7.2 and from 24.1 to 5.7. For the neat polymers, the effect of machining was less uniform. PLA showed almost no change in the parallel orientation (10.4 vs. 10.3) and only a moderate reduction in the perpendicular orientation (19.5 to 10.1). In contrast, ASA demonstrated a significant decrease, from 9.2 to 2.1 (parallel) and from 20.7 to 1.9 (perpendicular), achieving some of the lowest roughness values overall after machining. Overall, machining significantly

reduced Rq for all composites and for ASA, while PLA exhibited comparatively limited improvement, particularly in the parallel orientation.

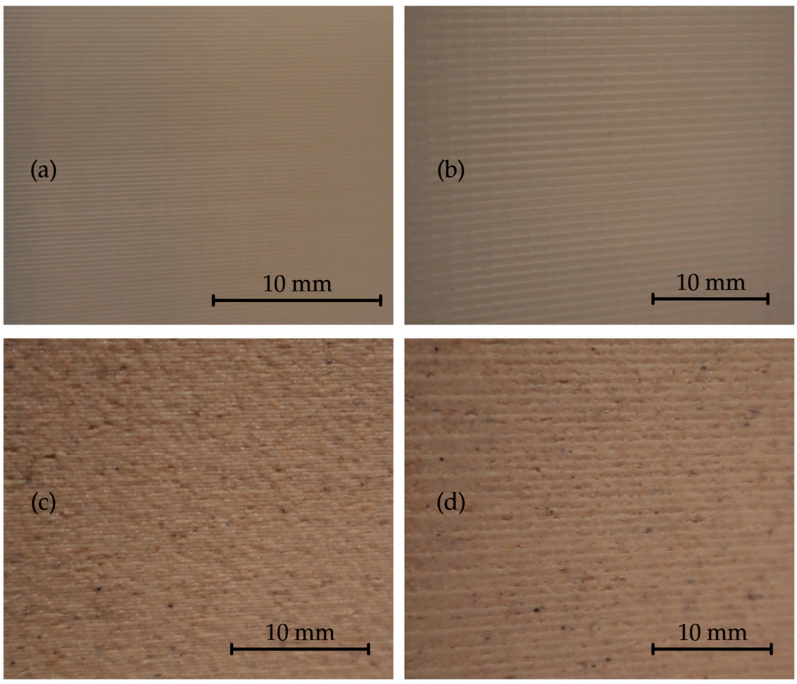

Figure 11. Visual comparison of non-machined test surfaces: (**a**)—PLA ⊥; (**b**)—PLA ∥; (**c**)—composite A ⊥; (**d**)—composite A ∥.

Other surface roughness results obtained during this study (Ra, Ry, Rz) are summarised in Table 5. While both Ra and Rq values for non-filled materials differ significantly, especially in β direction, similar values obtained for both average profile extremities (Rz) and the single highest profile extremity (Ry) in α direction suggest, as described above, that the measured surface roughness for neat polymers is mainly a result of the 3D printing process and not the material itself. The high Ry and Rz values obtained for all three composites, particularly for composite B printed parallel to the print bed (∥), indicate a substantial contribution of profile extremities to the measured surface roughness. Such extremities could be associated with wood particles protruding from the surface as well as with surface irregularities caused by the inclusion of those particles. The latter may include voids caused by insufficient interfacial adhesion or cavities caused by moisture release and off-gassing during processing. However, although the measured roughness parameters establish the presence of pronounced local profile extremities, their specific physical origins were not directly identified in this study. These explanations should therefore be regarded as plausible interpretations rather than experimentally verified mechanisms.

The comparison of machined and non-machined samples shows, similarly to the Rq results, a significant difference in both average roughness (Ra) and profile extremities (Ry, Rz) for all tested materials except PLA. Machining of the samples improved their surface quality significantly for all tested composites and ASA. In contrast, PLA did not exhibit a comparable improvement in surface quality after milling. In particular, the measured profile extremities (Ry and Rz) increased after machining, indicating that milling did not necessarily result in a smoother measured surface profile. Several factors may potentially contribute to this behaviour. Material removal may have exposed features associated with the layer-based structure of the printed part, while the thermal conditions generated during cutting may also have influenced the resulting surface. In addition, the applied cutting conditions may not have been optimal for PLA, as the surface quality of milled 3D-printed

PLA parts can depend on the selected machining parameters [24,25]. However, these explanations remain hypotheses, as the underlying mechanisms were not directly investigated in the present study. Further research involving systematic optimisation of machining parameters, monitoring of thermal conditions during cutting, and detailed characterisation of the machined surface is therefore needed to determine the factors responsible for the observed behaviour.

Table 5. Ra, Ry and Rz of the tested materials.

Material	Print Orientation	Ra [µm]			Ry [µm]			Rz [µm]		
		Machined	α	β	Machined	α	β	Machined	α	β
A	∥	6.0	15.8	9.6	60.9	116.9	83.2	39.6	92.0	56.6
	⊥	4.0	25.2	17.4	37.7	174.7	121.9	27.6	139.9	94.0
B	∥	2.1	17.6	15.1	37.6	151.4	114.7	21.6	115.6	86.3
	⊥	1.5	21.7	17.7	18.8	142.9	125.7	11.0	123.9	78.7
C	∥	5.8	13.3	10.9	39.8	105.2	76.5	33.7	88.0	59.5
	⊥	4.6	19.6	11.8	33.0	130.8	76.3	27.9	110.1	61.3
PLA	∥	8.1	8.6	4.8	52.2	53.0	33.1	47.1	48.9	25.8
	⊥	8.2	16.5	1.6	52.0	78.2	11.8	45.7	74.4	9.8
ASA	∥	1.7	6.7	3.6	15.3	55.5	17.6	11.0	48.8	13.6
	⊥	1.5	17.3	2.2	10.5	87.4	13.9	8.7	82.6	9.3

∥—surface parallel to the print bed; ⊥—surface perpendicular to the print bed.

4. Conclusions

The investigated wood–PLA composites exhibited lower tensile and flexural strength and modulus than neat PLA. The reduced mechanical performance is associated not only with the material composition but also with the characteristic internal structure of FDM-printed parts. Imperfect fusion between deposited strands, interlayer interfaces and internal voids were observed and may substantially affect the mechanical response of the printed composites. These findings also highlight the limitations of directly applying conventional material data and testing approaches to FDM-printed components and indicate the need for testing procedures that account for their layered and porous structure. In terms of surface quality, the results showed that the roughness of neat polymers was primarily related to the FDM printing process, suggesting that further improvement may be achieved through optimisation of the printing parameters. In contrast, the higher roughness observed for the wood–PLA composites indicates a substantial contribution of the heterogeneous material structure itself, arising from the incorporation of wood particles into the polymer matrix. The elevated Ry and Rz values, particularly for composite B, further demonstrate that the surface characteristics were strongly influenced by local profile extremities and irregularities, which may be related to protruding wood particles, material heterogeneity and structural discontinuities such as voids. However, further research would be needed to establish the underlying causes of these surface features.

CNC milling substantially improved the surface quality of all investigated wood–PLA composites, with pronounced reductions in surface roughness after machining. At the same time, the composites required lower cutting forces than the neat polymers under the investigated machining conditions. The combination of relatively high initial surface roughness, low cutting forces and substantial roughness reduction indicates that CNC milling can be an effective post-processing method for improving the surface quality of FDM-printed wood–PLA composites. However, the layered structure of the printed material should be considered when selecting machining parameters, as preliminary tests showed that milling close to layer boundaries may cause material tear-out and surface damage.

Author Contributions: Conceptualization, W.J., K.S. and P.B.; methodology, W.J. and K.S.; validation, K.S. and P.B.; formal analysis, W.J.; investigation, W.J.; resources, W.J., K.S. and P.B.; data curation, W.J.; writing—original draft preparation, W.J.; writing—review and editing, W.J., K.S. and P.B.; visualisation, W.J.; supervision, K.S. and P.B.; project administration, W.J. All authors have read and agreed to the published version of the manuscript.

Funding: This research received no external funding.

Data Availability Statement: The original contributions presented in this study are included in the article. Further inquiries can be directed to the corresponding authors.

Conflicts of Interest: The authors declare no conflicts of interest.

References

1. Ramaux, J.; Ziegler-Devin, I.; Besserer, A.; Nouvel, C. 3D Printing of Wood Composites: State of the Art and Opportunities. *Polymers* **2024**, *16*, 2827. [CrossRef] [PubMed]
2. Lalegani Dezaki, M.; Mohd Ariffin, M.K.A.; Ismail, M.I.S. Effects of CNC Machining on Surface Roughness in Fused Deposition Modelling (FDM) Products. *Materials* **2020**, *13*, 2608. [CrossRef] [PubMed]
3. Tao, Y.; Wang, H.; Li, Z.; Li, P.; Shi, S.Q. Development and Application of Wood Flour-Filled Polylactic Acid Composite Filament for 3D Printing. *Materials* **2017**, *10*, 339. [CrossRef] [PubMed]
4. Guessasma, S.; Belhabib, S.; Nouri, H. Microstructure and Mechanical Performance of 3D Printed Wood-PLA/PHA Using Fused Deposition Modelling: Effect of Printing Temperature. *Polymers* **2019**, *11*, 1778. [CrossRef] [PubMed]
5. Kariz, M.; Sernek, M.; Obućina, M.; Kuzman, M.K. Effect of Wood Content in FDM Filament on Properties of 3D Printed Parts. *Mater. Today Commun.* **2018**, *14*, 135–140. [CrossRef]
6. Krapež Tomec, D.; Schwarzkopf, M.; Repič, R.; Žigon, J.; Gospodarič, B.; Kariž, M. Effect of Thermal Modification of Wood Particles for Wood-PLA Composites on Properties of Filaments, 3D-Printed Parts and Injection Moulded Parts. *Eur. J. Wood Wood Prod.* **2024**, *82*, 403–416. [CrossRef]
7. Ayrilmis, N. Effect of Layer Thickness on Surface Properties of 3D Printed Materials Produced from Wood Flour/PLA Filament. *Polym. Test.* **2018**, *71*, 163–166. [CrossRef]
8. Zurnacı, E. Impact of Printing Parameters on the Surface Morphology and Thermal Stability of Sustainable FDM Filaments: A Taguchi-Based Factorial Design Study. *Appl. Sci.* **2026**, *16*, 2904. [CrossRef]
9. Wei, W.; Cong, R.; Xue, T.; Abraham, A.D.; Yang, C. Surface Roughness and Chip Morphology of Wood-Plastic Composites Manufactured via High-Speed Milling. *BioResources* **2021**, *16*, 5733–5745. [CrossRef]
10. Fiberlogy. *FiberWood: Technical Data Sheet*; Fiberlab S.A.: Brzezie, Poland, 2025.
11. Spectrum Filaments. *Spectrum WOOD: Technical Data Sheet*; Spectrum Group Sp. z o.o.: Pęcice Małe, Poland, 2022.
12. ROSA3D. *Filament 3D PLA Starter 1.75 mm: Technical Data Sheet*; ROSA PLAST Sp. z o.o.: Hipolitów, Poland, 2025.
13. ROSA3D. *Filament 3D BioWOOD 1.75 mm: Technical Data Sheet*; ROSA PLAST Sp. z o.o.: Hipolitów, Poland, 2025.
14. Fiberlogy. *Fiberlogy ASA: Technical Data Sheet*; Fiberlab S.A.: Brzezie, Poland, 2025.
15. Ellis, A. Ellis' Print Tuning Guide. Available online: https://ellis3dp.com/Print-Tuning-Guide/ (accessed on 24 September 2026).
16. *EN 323:1993*; Wood-Based Panels—Determination of Density. European Committee for Standardization (CEN): Bruxelles, Belgium, 1993.
17. *ISO 527-1:2019*; Plastics—Determination of Tensile Properties—Part 1: General Principles. International Organization for Standardization (ISO): Geneva, Switzerland, 2019.
18. *ISO 178:2019*; Plastics—Determination of Flexural Properties. International Organization for Standardization (ISO): Geneva, Switzerland, 2019.
19. *EN 15534-1:2014+A1:2017*; Composites Made from Cellulose-Based Materials and Thermoplastics (Usually Called Wood-Polymer Composites (WPC) or Natural Fibre Composites (NFC))—Part 1: Test Methods for Characterisation of Compounds and Products. European Committee for Standardization (CEN): Bruxelles, Belgium, 2017.
20. Farah, S.; Anderson, D.G.; Langer, R. Physical and Mechanical Properties of PLA, and Their Functions in Widespread Applications—A Comprehensive Review. *Adv. Drug Deliv. Rev.* **2016**, *107*, 367–392. [CrossRef] [PubMed]
21. 3D4Makers. *ASA Filament: Technical Data Sheet*; 3D4Makers: Haarlem, The Netherlands.
22. Tóth, C.; Kovács, N.K. Comparison of the Accuracy of Analytical Models for Basalt Fiber-Reinforced Poly(lactic acid) Composites Prepared by Injection Molding and Fused Filament Fabrication. *Int. J. Adv. Manuf. Technol.* **2022**, *121*, 3999–4010. [CrossRef]
23. O'Connor, L. Comparative Analysis of the Mechanical Properties of FDM and SLA 3D Printed Components. *J. Micromanuf.* **2025**, *9*, 214–228. [CrossRef]

24. El Mehtedi, M.; Buonadonna, P.; Carta, M.; El Mohtadi, R.; Marongiu, G.; Loi, G.; Aymerich, F. Effects of milling parameters on roughness and burr formation in 3D-printed PLA components. *Procedia Comput. Sci.* **2023**, *217*, 1560–1569. [CrossRef]
25. Lorenzoni, M.; Spitaels, L.; Riviere-Lorphevre, E.; Odent, J.; M'Saoubi, R.; Cloëz, L.; Fontaine, M.; Ducobu, F. Finish milling of polylactide (PLA) 3D-printed parts: Influence of printing pattern and lubrication on final surface roughness. *Mater. Res. Proc.* **2025**, *54*, 1747–1756. [CrossRef]

Disclaimer/Publisher's Note: The statements, opinions and data contained in all publications are solely those of the individual author(s) and contributor(s) and not of MDPI and/or the editor(s). MDPI and/or the editor(s) disclaim responsibility for any injury to people or property resulting from any ideas, methods, instructions or products referred to in the content.